

DATA DEPENDENT STABILITY OF FORWARD IN TIME AND CENTRED IN SPACE (FTCS) SCHEME FOR SCALAR HYPERBOLIC EQUATIONS

RITESH KUMAR DUBEY

Abstract. The main novelty of this note is the approach which is used to show that Forward Time and Centred in Space (FTCS) scheme is data dependent stable for scalar hyperbolic conservation laws. Note that FTCS is well known to be unconditionally unstable in von-Neumann sense. In this new approach, the ratio of consecutive gradients is used to classify the initial data region where FTCS is non-oscillatory and stable. Numerical results for 1D scalar and system test problems are given to verify the claim.

Key words. Numerical oscillations; von-Neumann stability; smoothness parameter; finite difference schemes; hyperbolic conservation laws.

1. Introduction

The notion of stability of a numerical scheme for the time dependent problems evolves around the induced spurious numerical oscillations especially at discontinuities. In the founding work, Courant-Friedrichs and Levy shown that for the convergence, a difference scheme must contains the physical domain of dependence of the partial differential equation [1]. In other words, they gave a necessary condition on the ratio of the spatial and time discretization steps for the stability of the difference scheme known as CFL condition. Later O'Brien, Hyman and Kaplan defined the stability of a difference scheme in terms of the growth of rounding errors [14]. In the seminal work [13], Lax and Richtmyer defined the stability using the uniformly boundedness of linear difference operator in the numerical scheme and gave the the necessary and sufficient condition for the convergence of linear schemes. One can summarize that the stability of a scheme ensures for the bounded growth of the solution. This becomes a significant requirement when it comes to approximate the solution of following scalar hyperbolic initial value problem

$$(1) \quad u(x, t)_t + g(u(x, t))_x = 0, \quad u(x, 0) = u_0(x).$$

This boundedness of numerical solution is required because the physical solution $u(x, t)$ of (1) satisfies the following maximum principle,

$$(2) \quad \min_x(u(x, 0)) \leq u(x, t) \leq \max_x u(x, 0), \quad \forall x \text{ and } t \geq 0.$$

If one consider a uniform grid with the spatial width h , time step k and denote the discrete mesh point (x_j, t_n) by $x_j = jh$, $j = 1, 2, \dots, N$ and $t_n = nk$, $k = 1, 2, \dots, M$. Then the CFL number for (1) can be defined as $C = \lambda \max_u |g'(u)|$ where $\lambda = \frac{k}{h}$ and $g'(u)$ is the characteristic speed associated with (1). It can be approximated

Received by the editors May 30, 2015 and, in revised form, September 27, 2016.
2000 *Mathematics Subject Classification.* 35R35, 49J40, 60G40.
This research was supported by DST India project #SR/FTP/MS-015/2011.

at the cell interface $x_{j+\frac{1}{2}}$ of the cell $[x_j, x_{j+1}]$ can be

$$(3) \quad a_{j+\frac{1}{2}} = \begin{cases} \frac{\Delta_+ g_j^n}{\Delta_+ u_j^n} & \text{if } \Delta_+ u_j^n \neq 0, \\ g_j' & \text{else.} \end{cases}$$

Starting from the work in [1], the CFL number has been an indispensable tool for defining the stability of numerical schemes. The linear von-Neumann stability analysis of a numerical scheme deduces a stability condition on the CFL number. Stronger non-linear stability conditions which ensure the boundedness requirement (2) in the numerical solution of (1) are also heavily dependent on the CFL number. For example upwind range condition, monotone stability [12, 2, 20], positivity preserving [8, 16] and total variation stability [6].

In fact, one needs to satisfy the CFL requirement i.e., $C \leq K$ where $K \in \mathbb{R}$ to devise any new stable scheme e.g., TVD schemes in [3, 9, 19], essentially non-oscillatory (ENO) schemes [7, 21], weighted essentially non-oscillatory schemes [24]. Apart from defining the stability, in a recent paper [10], the CFL number is exploited for the improved approximation by the flux limiters based scheme.

In this work, we consider the FTCS scheme obtained by the discretization of (1) by replacing the time derivative with a forward difference and the space derivative with a centred difference formula as

$$(4) \quad u_j^{n+1} = u_j^n - \frac{k}{2h} (g_{j+1}^n - g_{j-1}^n).$$

where $g_j^n = g(u_j^n)$ and $u_j^n \approx u(x_j, t_n)$. The above three point centred FTCS scheme (4) seems to be a correct and natural choice as the spatial discretization in FTCS does not violate the physical domain of dependence of (1). Contrary to the expectation, even for the linear problem $g(u) = au$, the solution obtained by FTCS scheme (4) is diverging and the induced oscillations grow exponentially no matter how small the time step is compared to the space step. The classical von-Neumann stability analysis also shows that FTCS (4) is unconditionally unstable. Moreover, FTCS does not satisfy criteria for any of the above mentioned non-linear stability conditions see [11]. One can find such unconditional instability of FTCS scheme (4) quite surprising mainly because as

- The FTCS (4) and the centered Lax-Wendroff (LxW) scheme [15] shares the same spatial stencil of grid points. Note that, for the CFL number $C = \lambda|a| \leq 1$, the three point centred LxW scheme is linearly stable [23] while FTCS is completely unstable.
- It can be observed that for smooth initial data, such as sinusoidal wave, the induced oscillations by FTCS does not grow immediately. Moreover, up to some extent, the occurrence of induced oscillations can be controlled by choosing small CFL number C , see Figure 2. On the other hand when applied on discontinuous initial data, FTCS introduces strong oscillations immediately see Figure 3(a).

These observations have been the motivation for the present study of the dependence of induced oscillations by the FTCS scheme (4) on data type and the CFL number. More precisely, we look for initial data type for which FTCS preserves the positivity, monotonicity and is local extremum diminishing stability properties. In order to carry out the analysis, we follow the idea used by the author in [4]. Note that the schemes analyzed in [4] are **stable** in the von-Neumann sense where as the FTCS scheme (4) considered in this work is **unconditionally unstable**.

In this work the classification is done in terms of ratio of consecutive gradients which is classically defined as (see [3, 10, 11, 23])

$$(5) \quad \theta_j^n = \begin{cases} \frac{\Delta_- u_j^n}{\Delta_+ u_j^n} & \text{if } a \geq 0, \\ \frac{\Delta_+ u_j^n}{\Delta_- u_j^n} & \text{if } a < 0, \end{cases}$$

where $a = g'(u)$ is wave speed associated with (1) and $\Delta_{\pm} u_j^n = \pm u_{j\pm 1} - u_j$. Rest of paper is organized as follows: In section 2 we define data dependent stability (DDS) and give bounds for FTCS scheme for scalar linear and non-linear hyperbolic conservation laws. In section 4, numerical results are given for 1D benchmark scalar and nonlinear system test cases. These results show that FTCS is DDS and introduces oscillations only for specific data type. Conclusion and future plan is summarized in section 5.

2. Data Dependent stable (DDS) schemes

For simplicity consider, the linear analog of (1) i.e., transport problem,

$$(6) \quad \frac{\partial}{\partial t} u(x, t) + a \frac{\partial}{\partial x} u(x, t) = 0, a \in \mathbb{R}$$

$$(7) \quad u_0(x) = f(x)$$

where $u = u(x, t)$ is a scalar field transported by flow of constant velocity a . The exact solution of linear transport equation is given by

$$(8) \quad u(x, t) = u_0(x \pm at).$$

Seemingly simple, the linear transport equation (6) has played a crucial role in the development of the numerical methods for general hyperbolic conservation laws. It is the closed form solution (8) which pave the way to analyze any new numerical scheme, devised for more complex non-linear hyperbolic problems for its convergence and stability. Considering the solution (8), it is natural to seek a numerical scheme which is stable in the sense that it does not induce spurious numerical oscillations. In case of two point schemes such non occurrence of induced oscillations in solution of the (6) can be ensured by a linear scheme,

$$(9) \quad u_j^{n+1} = \begin{cases} \alpha u_j^n + \beta u_{j-1}^n, & \text{if } a \geq 0, \\ \alpha u_j^n + \beta u_{j+1}^n, & \text{if } a \leq 0, \end{cases}$$

where $\alpha \geq 0, \beta \geq 0$ and $\alpha + \beta = 1$. Under such condition, the above scheme (9) is a convex combination of two point values of $u_i^n, i = j, j \pm 1$ therefore ensure that updated value u_j^{n+1} will be stable in the sense of the following local maximum principle

$$(10) \quad \begin{aligned} \min(u_j^n, u_{j-1}^n) \leq u_j^{n+1} \leq \max(u_j^n, u_{j-1}^n) & \quad \text{if } a \geq 0, \\ \min(u_j^n, u_{j+1}^n) \leq u_j^{n+1} \leq \max(u_j^n, u_{j+1}^n) & \quad \text{if } a \leq 0, \end{aligned}$$

Moreover the condition $\alpha + \beta = 1$ and $\beta = a \frac{k}{h} \geq 0$ ensure that (9) is a consistent approximation of (6). A simple von Neumann stability analysis shows (9) is stable provided $|a| \frac{k}{h} \leq 1$. The condition (10) also ensures that the computed solution satisfies the following discrete analog of the maximum principle (2)

$$(11) \quad \min_j \{u_j^0\} \leq u_j^{n+1} \leq \max_j \{u_j^0\}, \forall j = 1, 2, \dots, N \text{ and } \forall n = 1, 2, \dots, M.$$

Note that since scheme (9) is linear, its consistency and stability ensure for its convergence by Lax-Ritchmyer Theorem [13]. Considering above local maximum principle (10) and notion of data compatibility in [23] we define,

Definition 2.1. Consider a three point scheme written in the form

$$(12) \quad u_j^{n+1} = \begin{cases} \alpha(\theta_j)u_j^n + \beta(\theta_j)u_{j-1}^n & \text{if } a \geq 0 \\ \alpha(\theta_j)u_j^n + \beta(\theta_j)u_{j+1}^n & \text{if } a \leq 0, \end{cases}$$

where the coefficients α, β may depend on CFL as well as smoothness parameter (5). We call scheme (12) data independent stable if

$$(13) \quad \alpha_j \geq 0, \beta_j \geq 0 \text{ and } \alpha_j + \beta_j = 1 \quad \forall \theta_j \in \mathbb{R},$$

where $\alpha_j = \alpha(\theta_j), \beta_j = \beta(\theta_j)$. In case, (13) holds only for $\theta_j \in \mathbb{R} \setminus \mathbb{S}$ where $\mathbb{S} \subset \mathbb{R}$, scheme (12) is called data dependent stable.

3. DDS stability of FTCS for non-linear scalar problem

The sonic point u^* of (1) corresponds to zero wave speed i. e., $g'(u^*) = 0$ and signals a change in the wave direction. It is well known that in many numerical methods produces significant errors near sonic points, especially at expansive sonic points and lead to sonic expansion. There are standard approaches to avoid these difficulties such as Harten’s sonic entropy fix or addition of artificial viscosity [11]. Therefore we focus to analyse the bounds for FTCS (4) only in the non-sonic region to get non-oscillatory approximation of scalar problem (1).

Theorem 3.1. Away from the sonic point i.e., where $a_{j-\frac{1}{2}} \times a_{j+\frac{1}{2}} > 0$, the FTCS scheme (4) is data dependent stable and non-oscillatory in the solution region where

$$(14) \quad \theta_j^n \in \mathbb{S}_{FTCS} = \begin{cases} \left(\infty, -\frac{a_{j+1/2}}{a_{j-1/2}} \right] \cup \left[\frac{\lambda a_{j+1/2}}{2 - \lambda a_{j-1/2}}, \infty \right) & \text{if } g'(u) > 0, \\ \left(\infty, -\frac{a_{j-1/2}}{a_{j+1/2}} \right] \cup \left[-\frac{\lambda a_{j-1/2}}{2 + \lambda a_{j+1/2}}, \infty \right) & \text{if } g'(u) < 0. \end{cases}$$

provided $\lambda \max_u |g'(u)| \leq 2$.

Proof. Rewrite (4) using (3) as

$$(15) \quad u_j^{n+1} = u_j^n - \frac{\lambda}{2} \left(a_{j+\frac{1}{2}} \Delta_+ u_j^n + a_{j-\frac{1}{2}} \Delta_- u_j^n \right).$$

In case if $g'(u) > 0$ i.e., $a_{j\pm\frac{1}{2}} > 0$, (15) can be written in upwind form as

$$(16) \quad u_j^{n+1} = u_j^n - \frac{\lambda}{2} \left(\frac{a_{j+\frac{1}{2}} \Delta_+ u_j^n}{\Delta_- u_j^n} + a_{j-\frac{1}{2}} \right) \Delta_- u_j^n.$$

Rewriting it as

$$(17) \quad u_j^{n+1} = \alpha^+ u_j^n + \beta^+ u_{j-1}^n.$$

where the coefficients $\alpha^+ = 1 - \frac{\lambda}{2} \left(a_{j+\frac{1}{2}} \frac{\Delta_+ u_j^n}{\Delta_- u_j^n} + a_{j-\frac{1}{2}} \right)$ and

$\beta^+ = \frac{\lambda}{2} \left(a_{j+\frac{1}{2}} \frac{\Delta_+ u_j^n}{\Delta_- u_j^n} + a_{j-\frac{1}{2}} \right)$. Note that $\alpha^+ + \beta^+ = 1$, thus by definition (2.1), to

ensure non-oscillatory stable approximation such that $u_{j-1}^n \leq u_j^{n+1} \leq u_j^n$ by (15), it is sufficient that

$$(18) \quad \alpha^+ = 1 - \frac{\lambda}{2} \left(a_{j+\frac{1}{2}} \frac{\Delta_+ u_j^n}{\Delta_- u_j^n} + a_{j-\frac{1}{2}} \right) \geq 0, \text{ and } \beta^+ = \frac{\lambda}{2} \left(a_{j+\frac{1}{2}} \frac{\Delta_+ u_j^n}{\Delta_- u_j^n} + a_{j-\frac{1}{2}} \right) \geq 0.$$

Inequalities (18) satisfies if,

$$\frac{\Delta_+ u_j^n}{\Delta_- u_j^n} \geq -\frac{a_{j-\frac{1}{2}}}{a_{j+\frac{1}{2}}} \text{ and } \frac{\Delta_+ u_j^n}{\Delta_- u_j^n} \leq \frac{2 - a_{j-\frac{1}{2}} \lambda}{a_{j+\frac{1}{2}} \lambda}.$$

Which on inversion yield following non-oscillatory condition for FTCS scheme (26) in case of $g'(u) > 0$,

$$(19) \quad \frac{\Delta_- u_j^n}{\Delta_+ u_j^n} \leq -\frac{a_{j+\frac{1}{2}}}{a_{j-\frac{1}{2}}} \text{ OR } \frac{\Delta_- u_j^n}{\Delta_+ u_j^n} \geq \frac{a_{j+\frac{1}{2}} \lambda}{2 - a_{j-\frac{1}{2}} \lambda}$$

Similarly in case if $g'(u) < 0$ i.e., $a_{j+\frac{1}{2}} < 0$, $j = 1, 2, \dots$, (15) can be written as

$$(20) \quad u_j^{n+1} = u_j^n - \frac{\lambda}{2} \left(a_{j+\frac{1}{2}} + \frac{a_{j-\frac{1}{2}} \Delta_- u_j^n}{\Delta_+ u_j^n} \right) \Delta_+ u_j^n.$$

or

$$(21) \quad u_j^{n+1} = \alpha^- u_j^n + \beta^- u_{j+1}^n.$$

where $\alpha^- = \left(1 + \frac{\lambda}{2} \left(a_{j+\frac{1}{2}} + a_{j-\frac{1}{2}} \frac{\Delta_- u_j^n}{\Delta_+ u_j^n} \right) \right)$ and $\beta^- = -\frac{\lambda}{2} \left(a_{j+\frac{1}{2}} + a_{j-\frac{1}{2}} \frac{\Delta_- u_j^n}{\Delta_+ u_j^n} \right)$.

Since $\alpha^- + \beta^- = 1$, similar to above, (21) ensures for a non-oscillatory approximation provided,

$$(22) \quad \left(\frac{\lambda}{2} \left(a_{j+\frac{1}{2}} + a_{j-\frac{1}{2}} \frac{\Delta_- u_j^n}{\Delta_+ u_j^n} \right) \right) \geq -1 \text{ and } \frac{-\lambda}{2} \left(a_{j+\frac{1}{2}} + a_{j-\frac{1}{2}} \frac{\Delta_- u_j^n}{\Delta_+ u_j^n} \right) \geq 0.$$

Note that $\lambda a_{j+\frac{1}{2}} < 0$, therefore inequalities in (22) satisfy if

$$\left(\frac{\Delta_- u_j^n}{\Delta_+ u_j^n} \right) \leq \frac{-(2 + a_{j+\frac{1}{2}} \lambda)}{a_{j-\frac{1}{2}} \lambda} \text{ and } \frac{\Delta_- u_j^n}{\Delta_+ u_j^n} \geq -\frac{a_{j+\frac{1}{2}}}{a_{j-\frac{1}{2}}}$$

Since $\frac{-(2 + a_{j+\frac{1}{2}} \lambda)}{a_{j-\frac{1}{2}} \lambda} > 0$ and $\frac{a_{j+\frac{1}{2}}}{a_{j-\frac{1}{2}}} > 0$, thus on inversion above compound inequality satisfies if,

$$(23) \quad \frac{\Delta_+ u_j^n}{\Delta_- u_j^n} \leq -\frac{a_{j-\frac{1}{2}}}{a_{j+\frac{1}{2}}} \text{ OR } \frac{\Delta_+ u_j^n}{\Delta_- u_j^n} \geq \frac{-a_{j+\frac{1}{2}} \lambda}{(2 + a_{j+\frac{1}{2}} \lambda)}$$

□

Remark 1. Note that conditions (19) and (23) are equivalent to positivity or monotonicity preserving and local extremum diminishing stability [11, 8] of approximation by (17) and (21) respectively or equivalently by FTCS scheme (4). Moreover it can be shown that these conditions are sufficient to characterize the data region where FTCS is TVD. It follows from considering equations (16) and (20) along with the following result due to Harten [6]

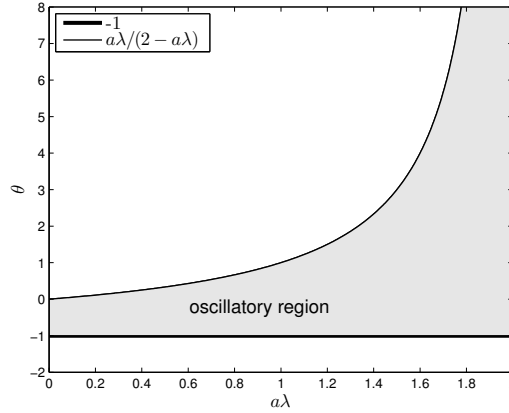


FIGURE 1. Plot θ v/s $a\lambda$, $a = 1$: $a\lambda \rightarrow 0$ stabilizes the FTCS as it corresponds to reduced oscillatory shaded region.

Lemma 3.2. Consider a conservative scheme in the form

$$(24) \quad \bar{u}_i^{n+1} = \bar{u}_i^n + C_{i+\frac{1}{2}} \Delta_+ \bar{u}_i^n - D_{i-\frac{1}{2}} \Delta_- \bar{u}_i^n.$$

A sufficient condition on coefficients C, D for the scheme (24) to be TVD is

$$(25) \quad C_{i+\frac{1}{2}} \geq 0, D_{i-\frac{1}{2}} \geq 0, 0 \leq C_{i+\frac{1}{2}} + D_{i-\frac{1}{2}} \leq 1.$$

For linear case i.e., $g(u) = au$ it follows from Theorem 3.1,

Corollary 3.3. The FTCS scheme for (6) i.e.,

$$(26) \quad u_j^{n+1} = u_j^n - \frac{ak}{2h} (u_{j+1}^n - u_{j-1}^n).$$

is data dependent stable and non-oscillatory in the solution data region where $\theta_j^n \in \mathbb{S}_{FTCS} = (\infty, -1] \cup \left[\frac{\text{sgn}(a)|a|\lambda}{2 - \text{sgn}(a)|a|\lambda}, \infty \right)$, provided CFL number $a\lambda \leq 2$.

In Figure (1) the non-oscillatory stability region \mathbb{S}_{FTCS} for (26) is given for $a > 0$. As $a\lambda \rightarrow 2$ the instability region goes to $+\infty$ making FTCS unstable for all data type except for those extrema where $\theta < -1$. On the other hand $a\lambda \rightarrow 0$ reduces the instability region in to $\theta \in [-1 : 0)$. It can easily be deduced from Figure 1 that it is better to use $a\lambda \leq 1$ so that second order FTCS gives non-oscillatory (stable) approximation for smooth data region where $\theta \approx 1$.

Remark 2. Note that this new approach, the data dependent stability analysis gives significant new information on data type and the stability of a scheme. Also, possibly this is the only approach which deduce a stability condition of FTCS scheme which fails to satisfy any existing notion of stability. This approach can be applied on linearly stable but oscillatory high order schemes to get further insight on the data region where one can retain higher accuracy as done in [4]. This data dependent stability approach can also be applied for stable numerical approximation of physically relevant convective dominated flow problems.

4. Numerical Verification

In order to validate numerically the data dependent stability of FTCS scheme, following two approaches are used. These hybrid methods using first order non-oscillatory Local Lax Friedrichs scheme [22] are designed to elaborate the data region which cause induced oscillations by FTCS. Let $F_{j+\frac{1}{2}}^{FTCS}$ and $F_{j+\frac{1}{2}}^{LLF}$ denotes the numerical flux function of FTCS and LLF scheme.

4.1. Stable hybrid Approach. To show FTCS does not introduces oscillations for data region \mathbb{S}_{FTCS} : This approach can be viewed as the following hybrid scheme

$$(27) \quad u_j^{n+1} = u_j^n - \lambda \left(\chi(\theta_j) \Delta_- F_{j+\frac{1}{2}}^{FTCS} + (1 - \chi(\theta_j)) \Delta_- F_{j+\frac{1}{2}}^{LLF} \right)$$

where χ is a limiting function defined as

$$(28) \quad \chi(\theta_j) = \begin{cases} 1 & \text{if } \theta_j \in \mathbb{S}_{FTCS} \\ 0 & \text{if } \theta_j \notin \mathbb{S}_{FTCS} \end{cases}$$

Results obtained by this approach are shown by legend 'FTCSLLF'.

Remark 3. Note that LLF scheme is TVD [23] and in the light of Remark 1 and Lemma 3.1, FTCS is conditionally TVD. Therefore, it follows that the hybrid scheme (27) is always TVD.

4.2. Unstable hybrid approach. To show FTCS introduces oscillations only for data region $\mathbb{R} \setminus \mathbb{S}_{FTCS}$: Results obtained by this approach are shown by legend 'FTLLFCS'.

$$(29) \quad u_j^{n+1} = u_j^n - \lambda \left(\chi(\theta_j) \Delta_- F_{j+\frac{1}{2}}^{LLF} + (1 - \chi(\theta_j)) \Delta_- F_{j+\frac{1}{2}}^{FTCS} \right)$$

where χ is defined in (28). One can see from the presented numerical results that FTCS scheme is data dependent stable as stated in Theorem 3.1.

Remark 4. It is needed to state that the limiting approach used in hybrid schemes (27) and (29) is entirely different from the approach of weighted average flux (WAF) approach in [23] or slope and flux limiter based TVD schemes [3, 10]. Note that in the WAF or TVD approaches a weight or limiting function is used to get new *hybrid numerical flux function* for a scheme whereas in the present approach, use of limiting function χ yields a *hybrid scheme* which switches between FTCS and LLF scheme. In other words (27) and (29) are *scheme limiter* based hybrid schemes.

4.3. Linear Case. Consider linear transport equation (2) along with the following initial conditions

$$(30) \quad u_0(x) = \sin(\pi x), \quad x \in [-1 : 1]$$

This initial condition is taken to show one of the observations i.e., effect of CFL number on induced oscillations by FTCS which motivated the present study. It can be clearly seen in Figure 2 that numerical oscillations disappear for small CFL number. This supports the result in Theorem 3.3 as $C \rightarrow 0$ reduces the region of oscillations of θ to $(-1,0)$ as shown in Figure 1. Following two initial conditions are taken to show the data dependent stability of FTCS using approaches 4.1 and 4.2.

$$(31) \quad u_0(x) = \begin{cases} 1 & \text{if } |x| \leq 1/3 \\ 0 & \text{else} \end{cases}, \quad x \in [-1 : 1].$$

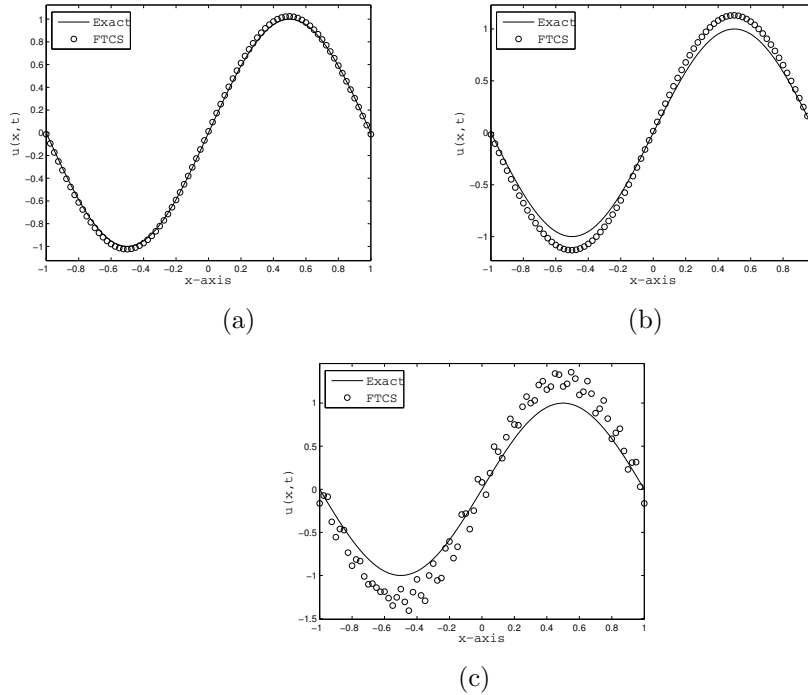


FIGURE 2. Effect of CFL on induced oscillations in the solution corresponding to (30), at $T = 4$ using $N = 80$ grid points (a) $C = 0.05$ (b) $C = 0.25$ and (c) $C = 0.5$.

$$(32) \quad u_0(x) = \begin{cases} \exp\left(\frac{-1}{1-x^2}\right) & \text{if } |x| \leq 1 \\ 0 & \text{else} \end{cases} \quad x \in [-2 : 4].$$

In Figure 3, 4 and Figure 5 numerical results are given using unstable FTCS, FTLLFCS and stable FTCSLLF schemes. Note that application of FTCS in its data dependent instability region (in approach FTLLFCS) introduces the oscillations while the stable approach FTCSLLF does not show any oscillation as FTCS is applied in its data dependent stability region. In Figure 4(b) numerical results are shown at large time $t = 12$ when the initial solution have travelled the periodic domain exactly six times.

4.4. Nonlinear scalar. Note that reduction of (4) using θ leads to non-conservative formulation (17) and (21). More precisely, keeping θ intact, scheme (17) and (21) can not be written in the form

$$(33) \quad u_j^{n+1} = u_j^n - \lambda[F_{j+\frac{1}{2}} - F_{j-\frac{1}{2}}]$$

where $F_{j+\frac{1}{2}}$ is the numerical flux function. Since the bounds for non-linear scalar case are obtained by these non-conservative approximations (17) and (21) therefore the hybrid numerical scheme 4.1, based these bounds can lead to wrong propagation of speed of shock. This can be avoided by using a simple and well established technique given in [17, 5] i.e., by using a conservative scheme in the neighbourhood of shock $\delta_{x_i}^{shock}$ with the help of a shock switch. Here neighbourhood of a shock point x_i is a discrete set of neighbouring point of the grid and we define it by

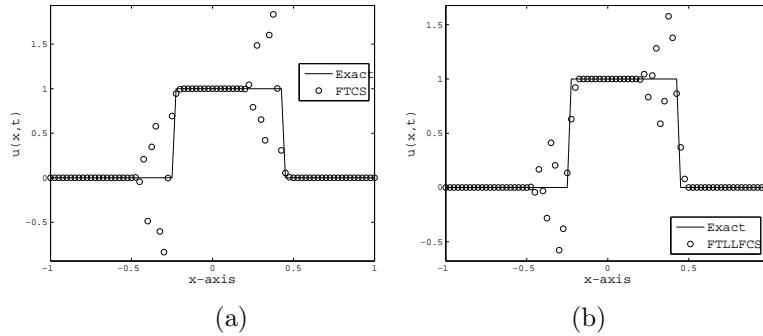


FIGURE 3. Solution corresponding to (31), with $N = 80$ grid point at $T = 0.1$ and $C = 0.6$, (a) FTCS is highly unstable but does not introduce oscillations for top and bottom of left and right discontinuity respectively (b) Induced oscillations by FTLLFCS approach, where FTCS is applied in its instability region $\theta \in \mathbb{S}_{FTCS} \setminus \mathbb{R}$.

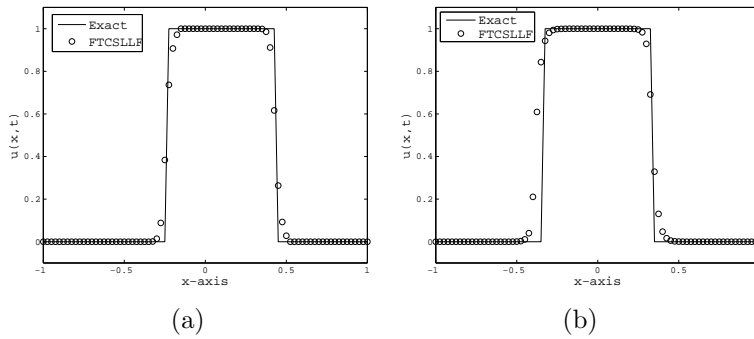


FIGURE 4. Non-oscillatory solution corresponding to (31) by FTCSLLF approach where FTCS is applied only in its stability region $\theta \in \mathbb{S}_{FTCS}$. Computed solutions using $N = 80$ grid point (a) $C = 0.6$ at time $T = 0.1$ and (b) $C = 0.8$ at time $T = 12$.

$\delta_{x_i}^{shock} = \{x_{i \pm k}, k = 1, 2, 3\}$. In the numerical results presented for non-linear case, a shock detector given in [28] is used to implement the stable hybrid approach 4.1. We consider the following two non-linear scalar Riemann problems given by

$$(34) \quad u_t + f(u)_x = 0,$$

(i) **Test problem 1:** Inviscid Burgers equation corresponds to the flux function

$$(35) \quad f(u) = \frac{u^2}{2},$$

with initial conditions

$$(36) \quad u_0(x) = \begin{cases} 1 & \text{if } x \leq 0.5 \\ 0 & \text{if } x > 0.5, x \in [0, 1]. \end{cases}$$

$$(37) \quad u_0(x) = \begin{cases} 1 & \text{if } |x| = 1/3 \\ 0 & \text{else, } x \in [-1, 1]. \end{cases}$$

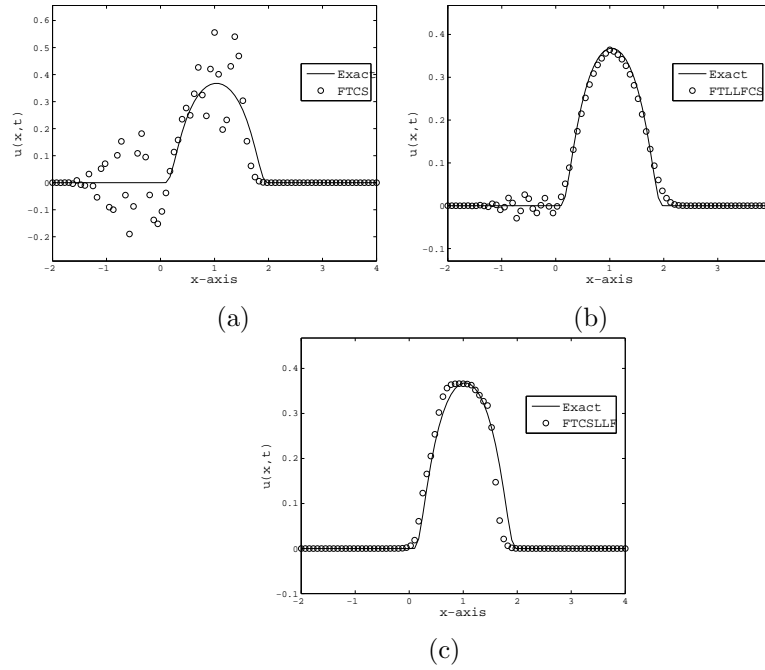


FIGURE 5. Solution corresponding to (32), at $T = 1.0$ and $C = 0.6$ (a) Highly oscillatory approximation by FTCS (b) Induced spurious oscillations by FTLFCS, FTCS introduce oscillation only in its instability region $\theta \in \mathbb{S}_{FTCS} \setminus \mathbb{R}$. (c) No oscillations by FTCSLLF approach.

$$(38) \quad u_0(x) = \frac{1}{4}(1 + \sin(\pi x)), x \in [-1 : 1]$$

Solution results for above test cases are given in Figures 6 to 9. Results in Figures 6 and 7 show that solution by FTCS and FTLFCS is oscillatory whereas FTCSLLF does not show numerical oscillations. The numerical solution by hybrid approach FTCSLLF is also compared with the solution by LLF corresponding to initial conditions (37) and (38) in Figure 8 and Table 1. Results in Figure 8 and Table 1 show that hybrid scheme FTCSLLF crisply captures the left rarefaction with higher resolution and gives faster convergence rate than the LLF scheme for smooth solution especially in L^∞ error norm.

TABLE 1. Comparison of order of accuracy for Burgers equations corresponding to IC (38) using $CFL = 0.2$ at pre-shock time $t = \frac{3}{4}Tb$.

N	LLF				FTCSLLF			
	L^1 Error	Rate	L^∞ Error	Rate	L^1 Error	Rate	L^∞ Error	Rate
10	1.0097e-01	...	9.8462e-02	...	6.5950e-02	...	1.3087e-01	...
20	4.7577e-02	1.0856	8.7008e-02	0.1784	2.0729e-02	1.6697	7.6180e-02	0.7806
40	2.4282e-02	0.9704	6.0629e-02	0.5211	6.9765e-03	1.5711	3.6201e-02	1.0734
80	1.2317e-02	0.9792	4.0273e-02	0.5902	2.8087e-03	1.3126	1.7531e-02	1.0461
160	6.2346e-03	0.9823	2.2895e-02	0.8148	1.2254e-03	1.1966	7.2388e-03	1.2761
320	3.1609e-03	0.9799	1.2646e-02	0.8564	6.7013e-04	0.8708	3.2286e-03	1.1648

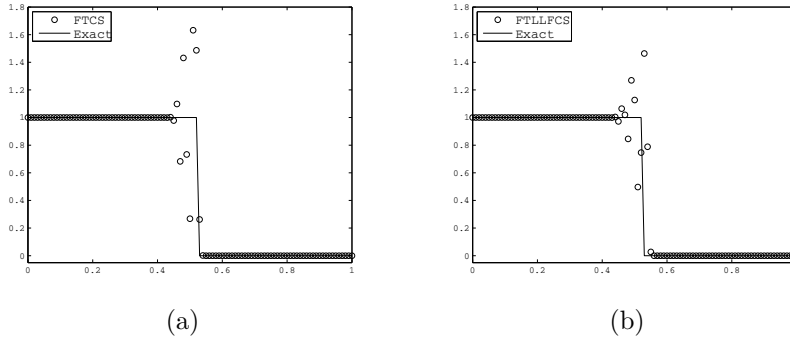


FIGURE 6. Solution of Burgers equation corresponding to IC (36) using $CFL = 0.8, N = 100$, at $T = 0.05$. In (a) and (b) Oscillatory solution by unstable FTCS scheme and FTLLFCS approach.

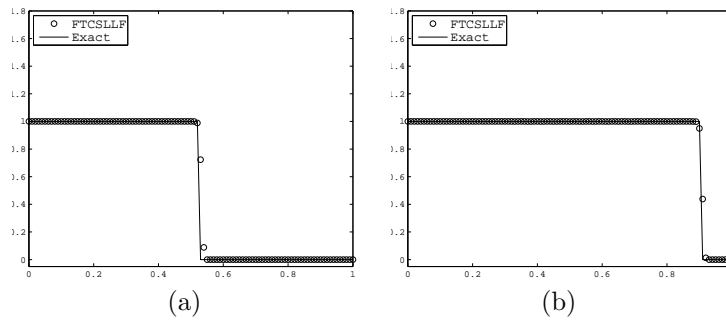


FIGURE 7. FTCSLLF approach gives stable non-oscillatory solution for Burgers equation test corresponding to IC (36) using $CFL = 0.8, N = 100$, at (a) $T = 0.05$ and (b) $T = 0.8$.

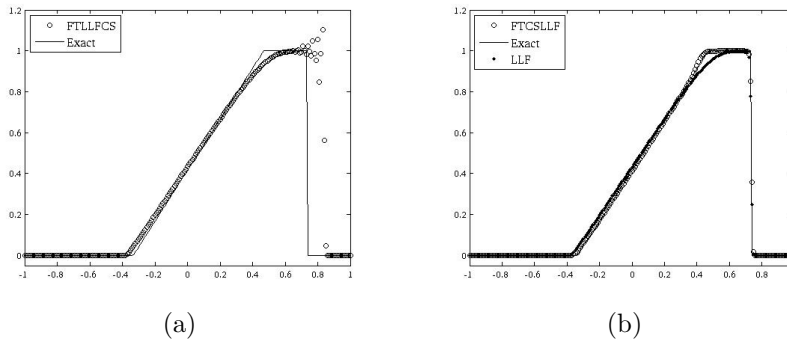


FIGURE 8. Solution of Burgers equation corresponding to IC (37) using $CFL = 0.4, N = 200$, at $t = 0.8$. (a) FTLLFCS gives oscillatory approximation for shock whereas (b) FTCSLLF give stable approximation for shock with out oscillations. The left rarefaction is correctly captured with high resolution compared to LLF.

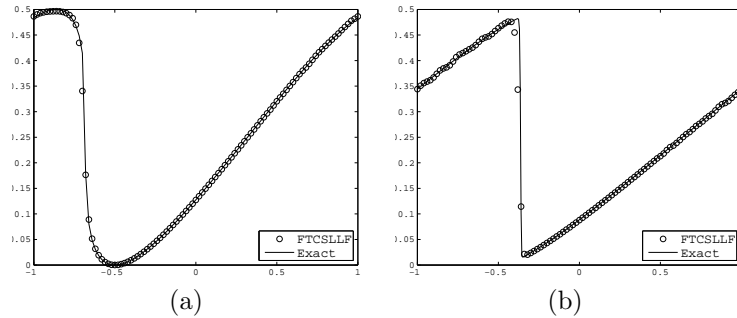


FIGURE 9. Solution of Burgers equation corresponding to IC (38) using $CFL = 0.25, N = 100$, at (a) breaking time $T_b = \frac{4}{\pi}$ (b) Solution at post breaking time $t = \frac{8}{\pi}$

(ii) **Test problem 2:** It corresponds to the flux function [22]

$$(39) \quad f(u) = \sin(u),$$

with initial condition with single discontinuity sitting at $x = 0$ and defined by

$$(40) \quad u_0(x) = \begin{cases} \frac{\pi}{4} & \text{if } x < 0, \\ \frac{15\pi}{4} & \text{if } x > 0. \end{cases}$$

The solution for this problem consists one stationary shock at $x = 0$ separated by rarefaction waves and one left moving shock. In Figure 10 numerical results obtained by stable FTCSLLF approach are given which shows an accurate capturing of steady shock and crisp resolution to rarefaction by FTCSLLF.

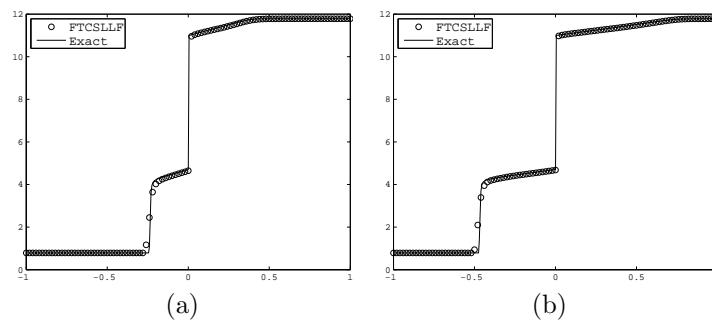


FIGURE 10. Solution of Riemann problem (39) corresponding to IC (40) using $CFL = 0.3, N = 100$, at time (a) $t = 0.5$ and (b) $t = 1.0$. Accurate approximation of stationary shock at $x = 0$ and crisp resolution for middle as well top rarefaction waves by FTCSLLF approach.

From the numerical results presented in Figure 3 to Figure 10 it can be concluded that FTCS is data dependent stable and does not introduce oscillations in the data region where $\theta \in \mathbb{S}_{FTCS}$. This also suggests that contrary to expectations and practice, FTCS can be used to

get non-oscillatory approximation by suitably hybridizing it with existing non-oscillatory schemes.

4.5. 1D Systems. We consider the Euler equation of Gas dynamics given by

$$(41) \quad \frac{\partial \mathbf{U}}{\partial t} + \frac{\partial \mathbf{F}}{\partial x} = 0$$

where vector $\mathbf{U} = \begin{bmatrix} \rho \\ \rho u \\ E \end{bmatrix}$ and $\mathbf{F} = \begin{bmatrix} \rho u \\ \rho u^2 + p \\ u(E + p) \end{bmatrix}$. The variables ρ, u, E represents density, velocity and energy of the system. The pressure p is related to conserved quantities through the equation of state. $p = (\gamma - 1)(E - \frac{1}{2}\rho u^2)$ with $\gamma = 1.4$. Since the hybrid scheme 4.1, is a centered, therefore the extension for the system (41) is straight forward and with out using any expansive Riemann solver. The characteristics speed for system (41) is approximated through

$$(42) \quad a_{i+\frac{1}{2}}^j = \begin{cases} \frac{F_{i+1}^j - F_i^j}{U_{i+1}^j - U_i^j} & u_{i+1}^j - u_i^j \neq 0 \\ \sigma(A_{i+\frac{1}{2}}) & \text{else,} \end{cases} \quad j = 1, 2 \dots l,$$

where $\sigma_{i+\frac{1}{2}}$ is the spectrum of eigen values of the flux Jacobian matrix $A_{i+\frac{1}{2}} = \mathbf{F}'(\mathbf{U})$. In above computation (42) the nonphysical discrete wave speed due to numerical overflow while $U_{i+1}^j \approx U_i^j$ are corrected using the wave speed correction technique proposed in [27].

4.5.1. Sod shock tube test [25]. Consider (41) with initial condition

$$(43) \quad (\rho, u, p) = \begin{cases} (1 \text{ kg/m}^3, 0 \text{ m/s}, 100,000 \text{ N/m}^2) & x < 0 \\ (0.125 \text{ kg/m}^3, 0 \text{ m/s}, 10,000 \text{ N/m}^2) & x \geq 0; \end{cases} \quad x \in [-10, 10].$$

In this test case the contact and shock are very close which cause a smeared approximation to the middle contact discontinuity. In Figure 11, Density, Pressure and velocity plots obtained by approach 4.1 are compared with Local Lax Friedrichs (LLF) scheme. Results show that FTCSLLF not only give oscillations free results but also yields much crisper resolution to the smooth rarefaction compared to LLF. Also contact discontinuity and moving shock is captured nicely at right location.

4.5.2. Lax shock tube test [29]. Consider 41 with initial condition

$$(44) \quad (\rho, u, p) = \begin{cases} (0.445 \text{ kg/m}^3, 0.698 \text{ m/s}, 3.528 \text{ N/m}^2) & x < 1, \\ (0.5 \text{ kg/m}^3, 0 \text{ m/s}, 0.571 \text{ N/m}^2) & x \geq 1; \end{cases} \quad x \in [0, 2].$$

Compared to Sod tube test, the shock in this case is very strong and many shock capturing schemes shows oscillatory approximation for it. In Figure 12 numerical results obtained by FTCSLLF are given and compared with LLF. It can be seen that that the method capture the contact and the rarefaction wave with higher resolution compared to LLF and does not show oscillations for strong shock.

4.5.3. Shu-Osher shock tube test [26].

$$(45) \quad (\rho, u, p) = \begin{cases} (3.857143, 2.629369, 10.3333) & x < -4.0, \\ (1 + 0.2 \sin(5x), 0, 1) & x \geq -4.0. \end{cases}$$

This test depicts shock interaction with a sine wave in density and the main challenge is to capture both the complex small-scale smooth flow and shocks. In Figure 13 results are presented an again compared with LLF scheme. It is evident from results that the FTCSLLF yields oscillation free approximation for shock with higher resolution compared to LLF for complex oscillatory solution region between

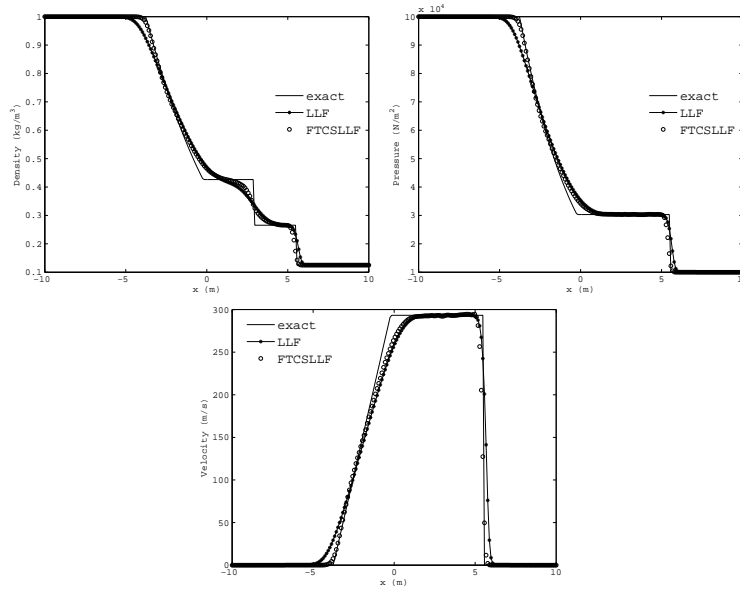


FIGURE 11. Solution plot for Sod shock tube problem, $N = 200$, $CFL = 0.45$

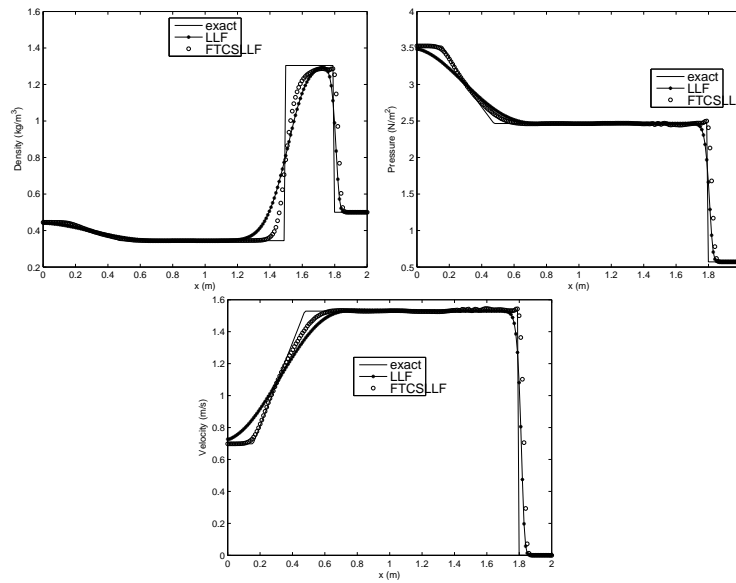


FIGURE 12. Solution plot for Sod shock tube problem, $N = 200$, $CFL = 0.45$

[0.5, 2.5]. It also capture the smooth region in around $[-3, 0.5]$ with out clipping or flattening error which is due to improved approximation of smooth extrema and steep gradient region.

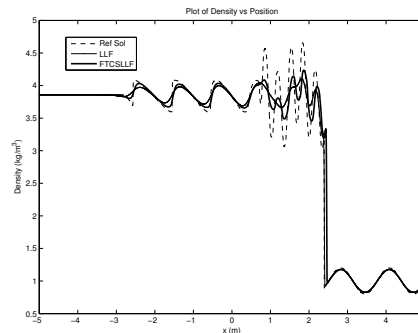


FIGURE 13. Numerical solution of shock density wave interaction $CFL = 0.8, N = 2000$ at time $t = 1.8$. High resolution of smooth extrema and steep gradient region.

5. Conclusion

A classification of data type is done to obtain non-oscillatory stability bounds on initial data profile for unconditionally unstable (in von-Neumann sense) FTCS scheme and also numerically verified. An extension of this preliminary study and idea of DDS for other existing schemes for non-linear hyperbolic problem is being carried out for a generalized separate work.

Acknowledgement

Author is thankful to the reviewers for their constructive comments and suggestions for inclusion of some numerical results which significantly helped to improve the over all presentation of the manuscript.

References

- [1] R. Courant, K. Friedrichs, and H. Lewy. On the partial difference equations of mathematical physics. *IBM J. Res. Dev.*, 11(2):215–234, March 1967.
- [2] M G Crandall and A Majda. Monotone difference approximations for scalar conservation laws. *Mathematics of Computation*, 34:1–21, 1980.
- [3] Ritesh Kumar Dubey. Flux limited schemes: Their classification and accuracy based on total variation stability regions. *Applied Mathematics and Computation*, 224:325–336, 2013.
- [4] Ritesh Kumar Dubey, Total variation stability and second-order accuracy at extrema *Electron. J. Diff. Eqns.,(EJDE)*, 20(2013), pp. 53-63.
- [5] Ritesh Kumar Dubey, A hybrid semi-primitive shock capturing scheme for conservation laws. *Electronic Journal of Differential Equations (EJDE)* , 19(2010), page 65-73.
- [6] Ami Harten. High resolution schemes for hyperbolic conservation laws,. *Journal of Computational Physics*, 49(3):357 - 393, 1983.
- [7] Ami Harten, Bjorn Engquist, Stanley Osher, and Sukumar R Chakravarthy. Uniformly high order accurate essentially non-oscillatory schemes, iii. *Journal of Computational Physics*, 71(2):231 – 303, 1987.
- [8] Antony Jameson. Positive schemes and shock modelling for compressible flows. *International Journal for Numerical Methods in Fluids*, pages 743–776, 1995.
- [9] Silvia Jerez and Mario Arciga. Switch flux limiter method for viscous and nonviscous conservation laws. *Applied Mathematics and Computation*, 246(0):292 – 305, 2014.
- [10] Friedemann Kemm. A comparative study of tvd-limiterswell-known limiters and an introduction of new ones. *International Journal for Numerical Methods in Fluids*, 67(4):404–440, 2011.
- [11] Culbert B. Laney. *Computational gasdynamics*. Cambridge University Press, 1998.

- [12] Peter D. Lax. Weak solutions of non-linear hyperbolic equations and their numerical approximation. *Communications in Pure and Applied Mathematics*, 7:159–193, 1954.
- [13] P. D. Lax and R. D. Richtmyer. Survey of stability of linear finite difference equations. *Communications on pure and applied mathematics*, 9(1956) 267-293.
- [14] O'Brien, G. G., Hyman M.A. and Kaplan S. A. A study of numerical solution of partial differential equations, *J. Math. Physics*, 29(1951) 223-251.
- [15] Peter D. Lax and Wendroff B. Systems of conservation laws. *Comm. Pure. Appl. Math.*, 13:217–237, 1960.
- [16] Peter D. Lax and Xu-Dong Liu. Solution of two-dimensional riemann problems of gas dynamics by positive schemes. *SIAM J. Sci. Comput.*, 19(2):319–340, March 1998.
- [17] Thomas Y. Hou and Philippe G. Lefloch. Why nonconservative schemes converge to wrong weak solutions: Error analysis. *Mathematics of Computation*, 62(206), 1994.
- [18] Philip G Lefloch and J G Liu. Generalized monotone schemes, discrete paths of extrema and discrete entropy conditions. *Mathematics of Computation*, 68:1025–1055, 1999.
- [19] William J. Rider. A comparison of tvd lax-wendroff methods. *Communications in Numerical Methods in Engineering*, 9(2):147–155, 1993.
- [20] R Sanders. On the convergence of monotone finite difference schemes with variable spatial differencing. *Mathematics of Computation*, 40:91–106, 1983.
- [21] Chi Wang Shu and Stanley Osher. Efficient implementation of essentially non-oscillatory shock-capturing schemes. *J. Comput. Phys.*, 77:439–471, August 1988.
- [22] R.J. Leveque. *Finite Volume Methods for Hyperbolic Problems*. Cambridge University Press, Cambridge, 2002.
- [23] E. F. Toro. *Riemann Solvers and Numerical Methods for Fluid Dynamics: A Practical Introduction*. Springer, 3rd edition, April 2009.
- [24] Yousef Hashem Zahran. An efficient {WENO} scheme for solving hyperbolic conservation laws. *Applied Mathematics and Computation*, 212(1):37 – 50, 2009.
- [25] G.A. Sod. Survey of several finite difference methods for systems of nonlinear hyperbolic conservation laws. *Journal of Computational Physics*, Apr 1978.
- [26] Shu Chi-Wang and Stanley Osher. Efficient implementation of essentially non-oscillatory shock-capturing schemes, ii. *Journal of Computational Physics*, 83:32–78, 1989.
- [27] S. Jaisankar and S.V. Raghurama Rao. A central rankinehugoniot solver for hyperbolic conservation laws. *Journal of Computational Physics*, 228(3):770 – 798, 2009.
- [28] M. Oliveira, P. Lu, X. Liu, and C. Liu. A new shock/discontinuity detector. *International Journal of Computer Mathematics*, 87(13):3063–3078, 2010.
- [29] Woodward, P., Colella, P.: The Numerical simulation of two-dimensional fluid flow with strong shocks. *Journal of Computational Physics* 54, 115-173 (1984).

Department of Mathematics and Research Institute, SRM University, Tamil Nadu, India
E-mail: riteshkumar.d@res.srmuniv.ac.in, riteshkd@gmail.com